Available online at www.sciencedirect.com
SCIENCE DIRECT®

Thermochimica Acta 402 (2003) 81–90

thermochimica acta

www.elsevier.com/locate/tca

Vibrational and structural evidence of phase transitions in some amides

Herman O. Desseyn [a,*], Katrien Clou [a], Jozef F. Janssens [a], Robert Carleer [b]

[a] *Department of Chemistry, RUCA, Groenenborgerlaan 171, B-2020 Antwerp, Belgium*
[b] *Department of Chemistry, LUC, Universitaire Campus, B-3590 Diepenbeek, Belgium*

Received 9 July 2002; received in revised form 1 November 2002; accepted 2 November 2002

Abstract

This article describes the vibrational evidence of reversible and irreversible phase transitions, observed in some simple amides RHNCOCONHR (R = alkyl or hydroxyethyl) and RHNCOCOOH (R = cyclopropyl).

Keywords: Phase transitions; ΔH_{vap} values; Vibrational spectra

1. Introduction

The concept of hydrogen bonding used to explain physical properties of some organic compounds and the formation of molecular aggregates [1,2] of small molecules has been extensively used as a model in some specific intermolecular interactions in bigger chemical systems [3].

Oxamides provide simple model substances to study the secondary amide function and the competition between the intermolecular versus intramolecular hydrogen bonding in these linear chain networks, that can form important supramolecular structures [4–6].

Oxamides form an important group of molecules in the vibrational characterisation of the amide bands [7–12] and for the symmetrical planar derivatives (RHNCOCONHR, R = H or alkyl group) the νCC is only Raman active and consequently not involved in the typical infrared fundamentals of the primary and secondary amide group. Oxamides are also interesting as ligands in coordination chemistry [13–18] and biologically applied systems [19–23].

For several years, our group has been engaged in the design of suitable oxamides, their complexes and their spectroscopic properties.

More recently we have published the thermal behaviour and the influence of hydrogen bonding on some physical constants in oxamides and thiooxamides [24,25]. In this article we describe the vibrational changes in the spectra observed by some reversible and irreversible phase transitions at high temperatures in some oxamide-like molecules.

2. Experimental

The synthesis of the investigated compounds has already been published in some previous articles [12,26,27].

Thermal analysis was performed on TA Instruments SDT 2960, TGA 2950 and DSC 2920. The

---

[*] Corresponding author. Tel. +32-3-218-0365; fax: +32-3-218-0233.
E-mail address: jojans@ruca.ua.ac.be (J.F. Janssens).

0040-6031/03/$ – see front matter © 2002 Elsevier Science B.V. All rights reserved.
PII: S0040-6031(02)00540-3

instruments were calibrated with standard methods: mass with two class A reference weights (100 mg and 1 g); temperatures with the melting point of indium, tin, lead and zinc; heat flow with the melting heat of indium. All experiments were performed under dry nitrogen (50 ml min^{-1}) and a heating rate of 5 K min^{-1}, except when stated otherwise in the text. All ΔH values are the average of three measurements.

The infrared spectra were recorded on a Bruker IFS 113v spectrometer using a liquid nitrogen cooled MCT detector with a resolution of 1 cm^{-1}. For each spectrum 100 scans were recorded and averaged.

The solid state Fourier Raman spectra were recorded on a Bruker IFS 66v interferometer equipped with a FT Raman FRA 106 module. The molecules were excited by the 1064 nm line of a Nd:YAG laser operating at 200 mW. For each spectrum 1000 scans were recorded and averaged. The variable temperature Raman spectra were recorded on a SPEX 1403 0.85-nm double-beam spectrometer. The molecules were excited by a Spectra Physics Model 2000 Ar^{+}-ion laser. A Miller–Harney cell was used to change the temperature. The spectra were recorded with a spectral slit of 4 cm^{-1}. For each spectrum three scans were recorded and averaged.

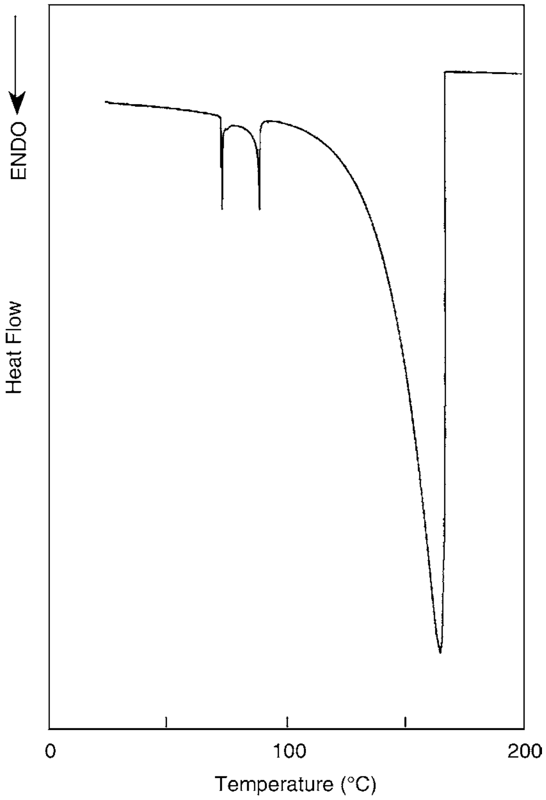

Fig. 1. DSC curve for *NN′*di-isobutyloxamide.

3. Results and discussion

3.1. Phase transitions

3.1.1. Phase transitions in NN′di-isobutyloxamide

The DSC curve for *NN′*di-isobutyloxamide is given in Fig. 1 ($\Delta H_{\mathrm{vap}} = 113$ kJ mol^{-1}). By heating the compound we observe two phase transitions in the solid state at respectively 72.5 and 88.0 °C. The reversibility of these transitions is given in Fig. 2.

The total energy of the two phase transitions has been calculated to be 2.76 kJ mol^{-1} in the heating and 2.95 kJ mol^{-1} in the cooling mode. The temperatures of the maxima in these phase transitions are 72.6 and

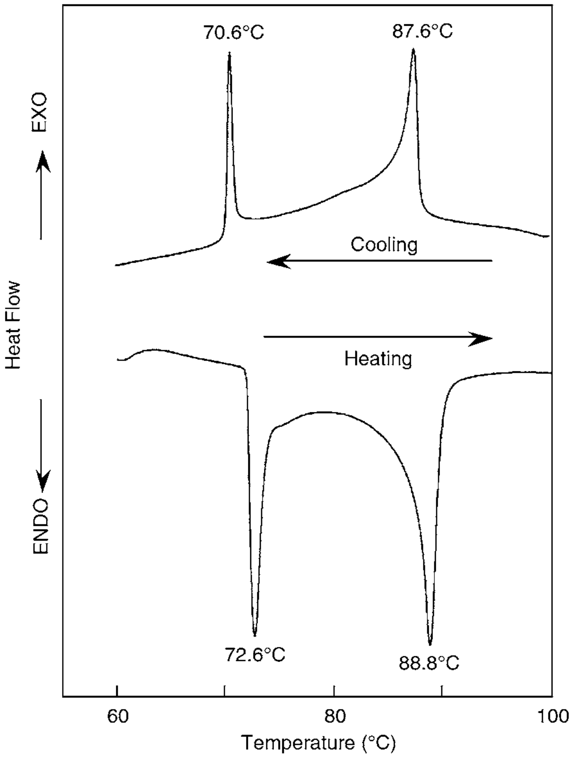

Fig. 2. Reversible phase transitions for *NN′*di-isobutyloxamide.

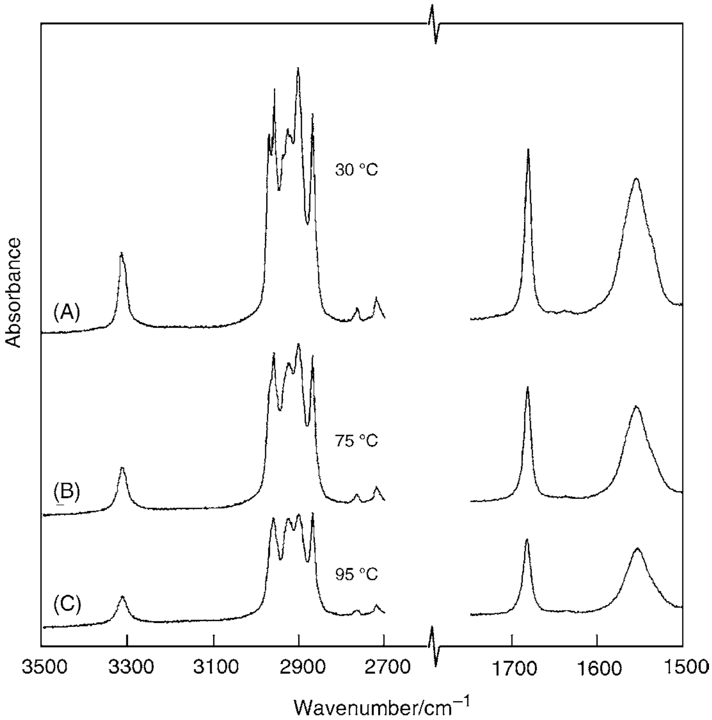

Fig. 3. Solid state Raman spectra of *NN′*di-isobutyloxamide at different temperatures: (A) 30 °C, (B) 75 °C, (C) 95 °C.

88.8 °C in the heating process and at 87.6 and 70.6 °C, respectively, in the cooling process. The difference in energy between the ΔH values in the heating and the cooling modes are within the error of the measurements. The slightly lower temperatures observed in the maxima the cooling mode is due to undercooling which is typical for a very pure compound.

Fig. 3 gives the Raman spectra of the compound at respectively 30 °C (A) (i.e. before the first transition), 75 °C (B) (between the two transitions) and at 95 °C (C) (after the second transition).

From this figure we can see that the νNH (3314 cm^{-1}) and the amide I (1699 cm^{-1}) and amide II modes (1555 cm^{-1}) are practically not changed indicating the same solid state structure for the amide part of the molecule (see Fig. 4). The small decrease of the νNH (3314–3312 cm^{-1} at 95 °C) and increase of νCO (1682–1684 cm^{-1} at 95 °C) may be ascribed to the very small change in the intermolecular distances, resulting in weaker intermolecular hydrogen bonding at higher temperatures [22]. The main differences in these spectra are observed in the νCH region (3000–2850 cm^{-1}) indicating a change in the geometry of the isobutyl groups in these phase transitions.

3.1.2. Phase transitions in *NN′*di-hydroxypropyloxamide

In a previous article [26] we reported on the vibrational analysis of some hydroxyalkyl substituted oxamides. The vibrational spectra indicated amide–amide hydrogen bonding comparable with the hydro-

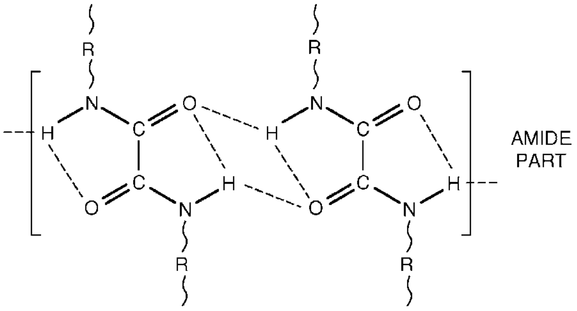

Fig. 4. Configuration of the “amide part” of the oxamides.

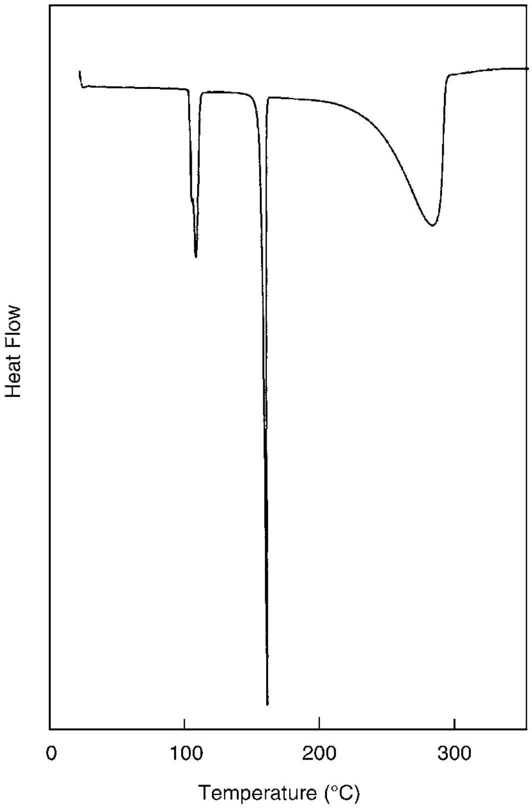

Fig. 5. DSC curve for *NN′*di-hydroxypropyloxamide.

gen bond pattern in the alkyloxamides and hydrogen bonding between the hydroxyl groups, dependent on the length of the alkyl substituent.

Fig. 5 gives the DSC curve of *NN′*di-hydroxypropyloxamide. By heating this compound we measure overlapping reversible phase transitions at 106 and 110 °C (16.7 kJ mol^{-1}) the melting at 160 °C (30.27 kJ mol^{-1}) and the boiling and partial decomposition process at 294 °C (135 kJ mol^{-1}).

Fig. 6 shows the Raman spectra of the compound in the 3500–2650 cm^{-1} region at 25 °C (A) and 115 °C (B) after the phase transitions and before the melting.

In the spectrum at 25 °C we can observe the νOH as a shoulder on the high frequency side of the intense νNH at 3315 cm^{-1} and the νCH region 3000–2850 cm^{-1}. However, after the transitions, the spectrum at 115 °C shows broad unprofiled bands even in the νOH and νNH region. These new broad profiles could very well be ascribed not only to the change in the alkyl group but also in the amide and

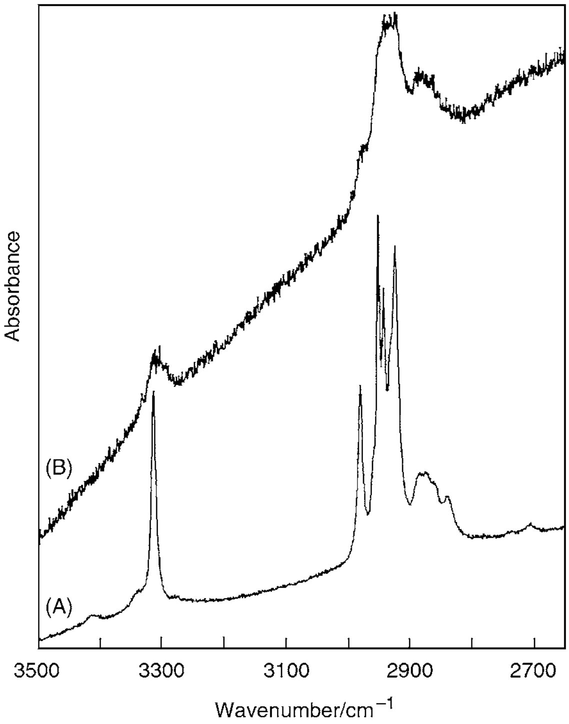

Fig. 6. Solid state Raman spectra of *NN′*di-hydroxypropyloxamide at different temperatures.

OH part of the molecule as can be observed from the bands in the 3300 cm^{-1} region.

The high energy (16.7 kJ mol^{-1}) involved in the transitions compared with the transition in the isobutyl compound (2.76 kJ mol^{-1}) indicates a greater change in the solid structure. The change in the alkyl group also changes the intermolecular –O–H · · · O hydrogen bonds, resulting in a different energy and according to the vibrational spectra a change in the solid compound.

The reversibility of the process, after the melting is shown in Fig. 7. The energy involved in the phase transition and the melting in the heating process (16.7 and 30.3 kJ mol^{-1}) and the cooling process (15.7 and 30.3 kJ mol^{-1}) are very well comparable. In the cooling process we measured an undercooling on solidification of about 7 °C, which is normal for a very pure compound. The temperature difference of the phase transition is about 30 °C.

This temperature difference of the transitions in the heating and the cooling processes, the energy involved

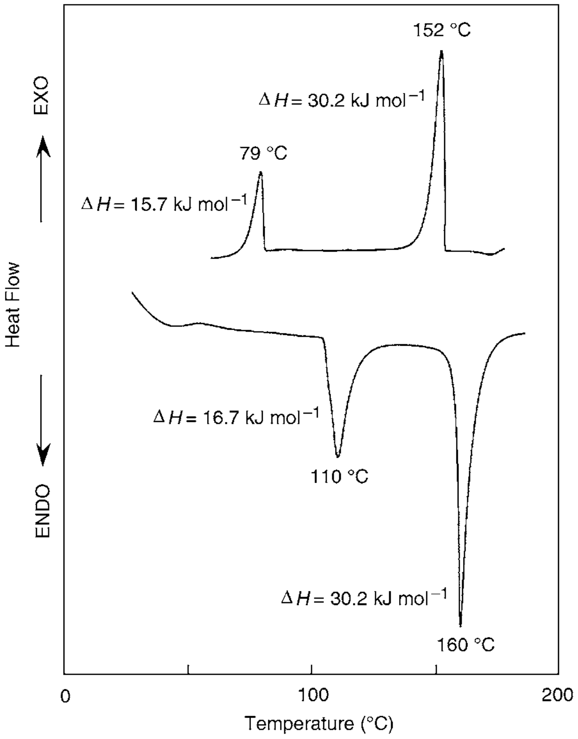

Fig. 7. Reversible phase transition for *NN*′di-hydroxypropyloxamide.

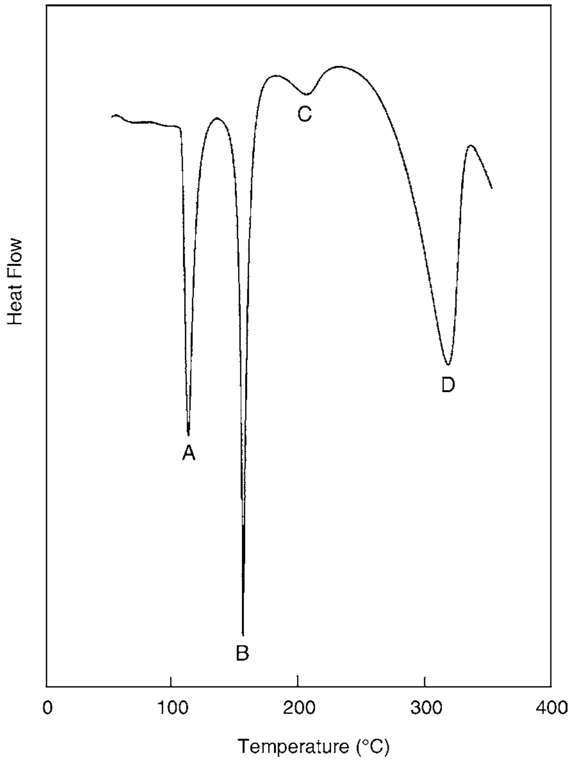

Fig. 8. DSC curve for *NN*′di-hydroxypentyloxamide.

in these phase transitions and the great differences in the spectra all indicate that the change in the solid state involves much more than a re-organisation of the alkyl chain as observed for the isobutyl compound.

3.1.3. Phase transitions in NN′di-hydroxypentyloxamide

Fig. 8 shows the DSC curve of *NN*′di-hydroxypentyloxamide crystallised from CH_2Cl_2. Four different endothermal processes occur in this 25–400 °C range. Transition A is a reversible phase transition, very well comparable with the first phase transition described for the isobutyl compound, transition B is the melting of the compound, comparable in temperature and energy with the hydroxypropyl compound. However, after the melting a third endothermal process (process C, indicated in Fig. 8) occurs at about 208 °C (5.4 kJ mol^{-1}) also without loss of weight, this is consequently a phase transition in the liquid state. The last endothermal process (75 kJ mol^{-1}) is the boiling and partial decomposition of the compound (residual mass 8%).

Fig. 9 shows two infrared spectra of the compound at 25 °C. Spectrum A gives the spectrum of the original compound at 25 °C. After heating the compound to 120 °C (i.e. behind the first transition in the solid) and cooling to 25 °C a spectrum identical to spectrum A has been obtained, indicating a reversible transition at 113 °C. After heating the compound to 175 °C (i.e. behind the melting process) and cooling to 25 °C, again a spectrum identical to spectrum A has been obtained, indicating that the compound crystallises from the liquid, in the same structure as obtained on crystallisation from a solvent (CH_2Cl_2). However, after heating to 220 °C (i.e. after the endothermal process C) and cooling to 25 °C we obtained a spectrum B as given in Fig. 9. The DSC curve of this compound exhibits two reversible phase transitions at respectively 75.7 and 85.0 °C, the melting process at 155 °C and no phase transition in the liquid state.

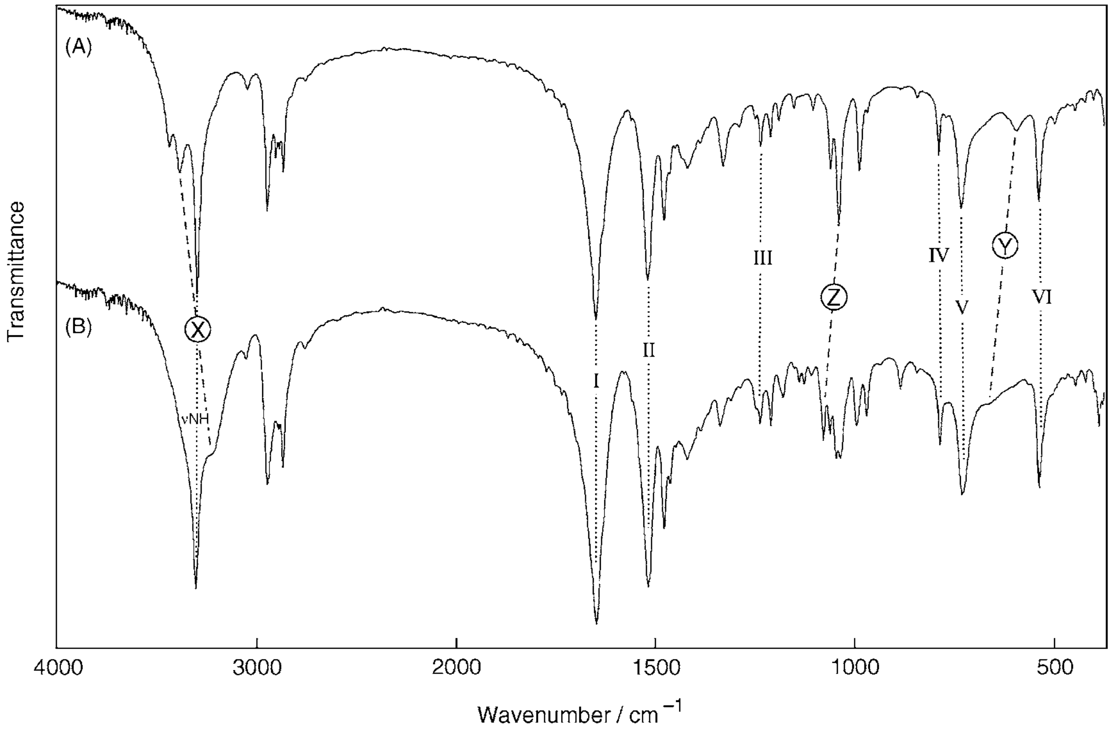

Fig. 9. Infrared spectra of *NN′*di-hydroxypentyloxamide at different temperatures.

The fact that for both compounds A and B the melting points practically coincide can be explained by the fact that the melting process is mainly a change in the amide part of the crystal structure and from the infrared spectra we clearly can conclude that these amide parts are identical in their inter- and intramolecular structure.

We re-crystallised the compound with spectrum B from CH_2Cl_2 and obtained again spectrum A, indicating that the molecular structure after transition C was not changed, but that process C involves an irreversible phase transition in the liquid phase.

So the difference in the spectra A and B must be due to the irreversible phase transition C.

From these spectra we clearly see that the νNH (3301 cm^{-1}) and the amide I (1646 cm^{-1}), amide II (1516 cm^{-1}), amide III (1245 cm^{-1}), amide IV (787 cm^{-1}), amide V (broad band at 732 cm^{-1}) and amide VI (537 cm^{-1}), indicated in Fig. 9 as νNH and I–VI, respectively, are identical in profile and frequency for A and B. This indicates an identical structure in the amide part for the two compounds (see Fig. 10).

The main difference is the position in the νOH mode, which appears as a split band (3434 and 3381 cm^{-1}) on the high frequency side of the intense νNH band for compound A and as a shoulder on the low frequency side (3223 cm^{-1}) of the νNH mode in compound B (X in Fig. 9).

The frequency shift of this νOH mode to lower frequency indicates a stronger O–H···O bonding in compound B. This stronger hydrogen bonding is further proved by the change of the πOH, located as a separate broad band at 592 cm^{-1} (band Y in Fig. 9) for compound A and appearing as a shoulder (680 cm^{-1}) on the low frequency side of the amide V mode in compound B. The change in the O–H bond strength should also be reflected in the νC–O(H) appearing in the 1050 cm^{-1} region. This νC–O(H) fundamental appears for compound A at 1038 cm^{-1} (Z in Fig. 9) and at 1077 cm^{-1} for compound B. The stronger O–H bond results in a weaker C–O(H) bond in compound

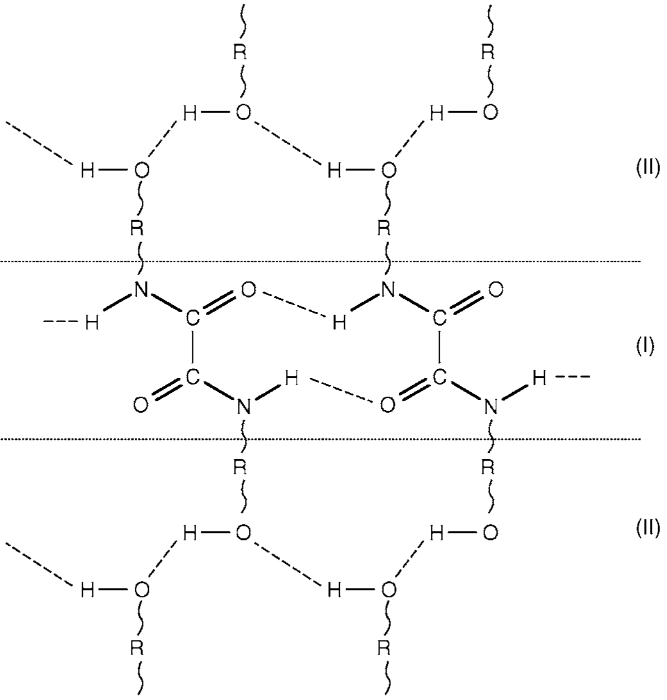

Fig. 10. Configuration of the “amide part” and “hydroxyalkyl part” of the oxamides.

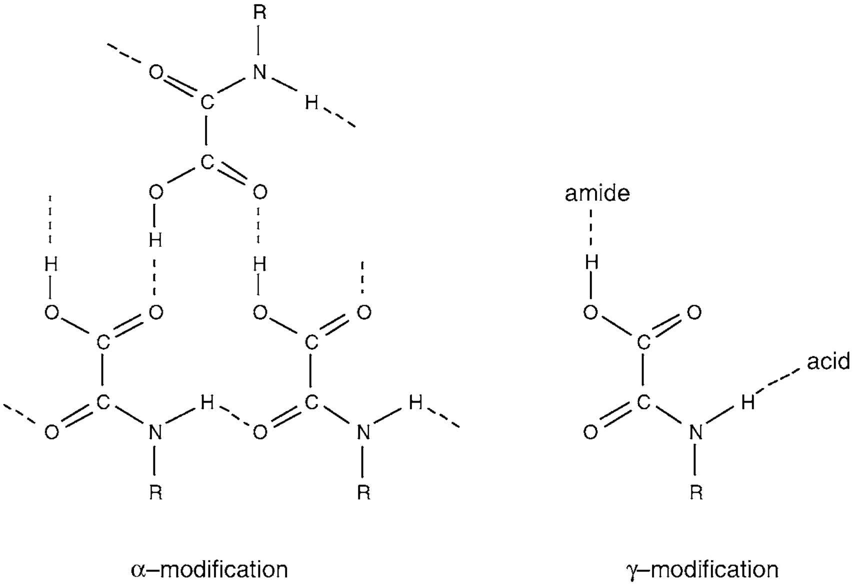

Fig. 11. The α- and γ-modifications of oxamic acids.

A compared with B. The spectroscopic prove of this change in hydrogen bonding (i.e. the assignments) is further confirmed by the spectra of the OD-deuteriated compounds.

As a conclusion we can state that the third endothermal reaction at about 208 °C consists of a change in the O–H···O intermolecular hydrogen bonding resulting in a much stronger interaction. This stronger hydrogen bonding also remains on cooling and condensation and results in a different spectrum B with the same structure in the amide group (indicated as I in Fig. 10), and a different interaction in the hydroxyalkyl region (indicated as II in Fig. 10).

By dissolving this compound in CH_2Cl_2 the strong O–H···O bonding is relieved and crystallisation of the product again results in the formation of the original compound A exhibiting less strong O–H···O hydrogen bonding.

3.1.4. Phase transitions in N-cyclopropyloxamic acid

In the vibrational analysis of *N*-alkyloxamic acids [27] we reported two different types of hydrogen bonded systems, depending on the alkyl substituent. In the α-modification we observed an acid–acid catamer and the typical amide–amide hydrogen bonded systems. In the γ-modification a heterogeneous acid–amide catamer configuration has been proposed from the vibrational analysis (Fig. 11). The cyclopropyl derivative crystallises at room temperature from CH_2Cl_2 mainly in the α-modification.

The DSC curve given in Fig. 12 shows five endothermal reactions. A, B and C are phase transitions in the solid state, D is the melting process and E is the boiling and partial decomposition of the compound.

Fig. 13 gives the infrared and Raman spectra in the 3400–3150 cm^{-1} region (νNH and νOH region) at different temperatures covering the three phase transitions A, B and C.

At room temperature we observe the νOH as a well-separated and intense band in the Raman spectrum at 3357 and at 3353 cm^{-1} in the infrared. A broad band at 3189 cm^{-1} in infrared and at 3197 cm^{-1} in Raman indicates the νNH mode in the α-modification.

At 3290 cm^{-1} a broad and slightly weaker band is observed in the infrared spectrum, which can be ascribed to the presence of some γ-modification at this low temperature. A cooling of the compound to −196 °C only results in a splitting of this band indicating also the presence of the acid and amide overtones and combination bands in this region. However, this broad band is also observed in the Raman spectrum and can consequently not be described to overtones or combinations of the amide and acid fundamentals.

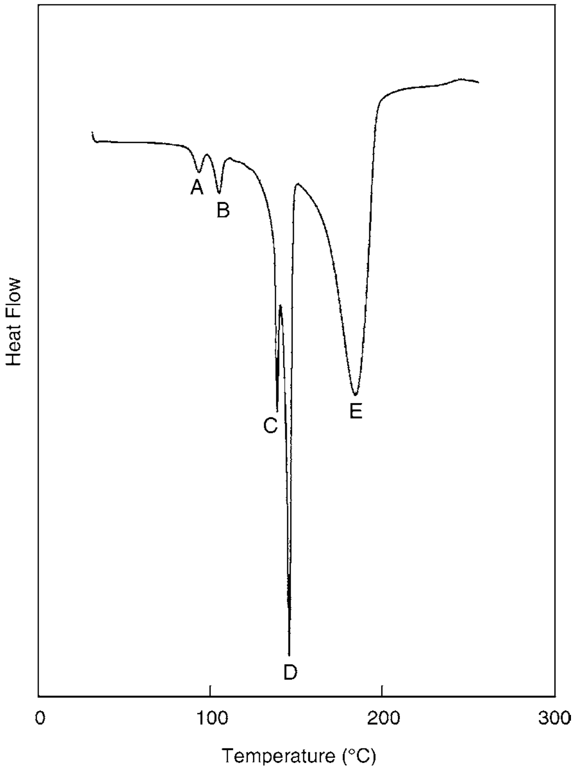

Fig. 12. DSC curve for *N*-cyclopropyloxamic acid.

Both in infrared and Raman we observe a gradual disappearance of these νOH and νNH modes and an increased intensity of the 3290 cm^{-1} band at 139 °C. The γ-modification has been completely formed where the νNH and the νOH modes in the acid–amide hydrogen bonded system coincide in the same region.

The decrease in the OH bond strength and the increase in the NH bond strength in the α → γ-modification is also reflected in the increase (1757 → 1763 (cm^{-1})) of the νCO (acid) mode and the decrease (1682 → 1679 (cm^{-1})) of the amidic νCO mode by increasing temperature (see Fig. 14).

The total energy involved in these irreversible solid state phase transitions is about 3 kJ mol^{-1} and is a good measure for the difference in the hydrogen bonding strength between the α- and γ-modifications.

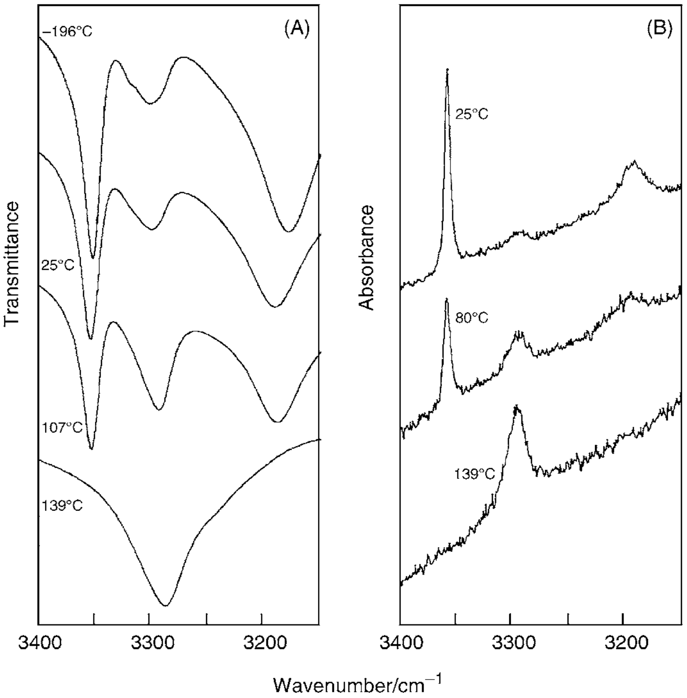

Fig. 13. Infrared (A) and Raman (B) spectra in the 3400–3150 cm^{-1} region of *N*-cyclopropyl oxamic acid at different temperatures.

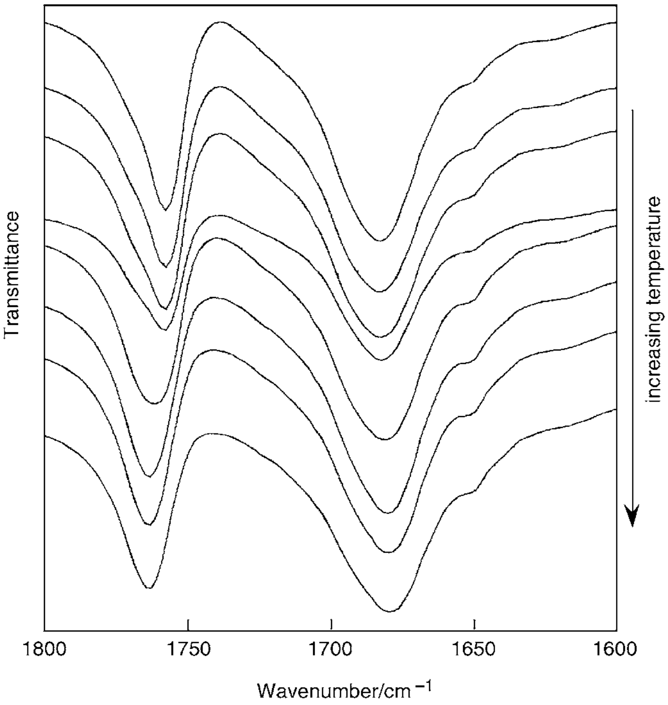

Fig. 14. Infrared spectra of *N*-cyclopropyloxamic acid in the 1800–1600 cm^{-1} region at different temperatures.

Acknowledgements

The authors thank Greta Thijs for technical assistance.

References

[1] L. Pauling, The Nature of the Chemical Bond, Cornell University Press, Ilhaca, NY, 1960.
[2] S.M. Reutzel, M.-C. Etter, J. Phys. Org. Chem. 5 (1992) 44.
[3] C. Huang, L.A. Cabell, E.A. Anslyn, J. Am. Chem. Soc. 116 (1994) 2778.
[4] S. Subramanian, M.J. Zaworotko, Coord. Chem. Rev. 137 (1994) 357.
[5] C.B. Aakeroöy, K.R. Seddon, Chem. Soc. Rev. 22 (1993) 397.
[6] Spek A.L. Platon, An integrated tool for the analysis of the results of a single crystal structure determination, Acta Cryst. 46A (1990) C-34.
[7] T.A. Scott, E.L. Wagner, J. Chem. Phys. 30 (1959) 465.
[8] L. Kahovec, J. Wagner, Z. Phys. Chem. B49 (1961) 156.
[9] T. Miyazawa, J. Chem. Soc. Jpn., Pure Chem. Sect. 75 (1954) 86.
[10] T. Miyazawa, T. Shimanouchi, S.I. Mizushima, J. Chem. Phys. 24 (1956) 413.
[11] D.B. Larson, S.P. McGlynn, J. Mol. Spectrosc. 47 (1973) 469.
[12] H.O. Desseyn, B.J. van der Veken, M.A. Herman, Spectrochim. Acta 33A (1977) 633.
[13] H. Ojima, K. Aymada, Bull. Chem. Soc. Jpn. 43 (1970) 1601, 3018.
[14] K. Nonoyama, H. Ojima, M. Nonoyama, Inorg. Chim. Acta 20 (1976) 127.
[15] G. Schoeters, H.O. Desseyn, Trans. Met. Chem. 6 (1981) 305.
[16] H.O. Desseyn, G. Schoeters, Bull. Soc. Chim. Belgium 95 (1985) 1, 13.
[17] F.J. Quaeyhaegens, S.P. Perlepes, H.O. Desseyn, Spectrochim. Acta 45A (1989) 8, 809.
[18] W. Van Riel, H.O. Desseyn, W. Van de Mieroop, A.T.H. Lenstra, Trans. Met. Chem. 5 (1980) 330.
[19] R.E. Gilmore, G.K. Pagenkoph, Inorg. Chem. 24 (1985) 2436.
[20] Y. Jounaux, J. Sletten, O. Kahn, Inorg. Chem. 24 (1985) 4063.
[21] Y. Journaux, J. Sletten, O. Kahn, Inorg. Chem. 24 (1986) 439.
[22] F. Lloret, K. Nakatani, Y. Journaux, O. Kahn, Y. Pei, J.P. Renard, J. Chem. Soc., Chem. Commun. (1988) 642.
[23] Y. Pei, O. Kahn, J. Sletten, J.P. Renard, R. Georges, J.C. Gianduzzo, J. Curley, Q. Xu, Inorg. Chem. 27 (1988) 47.
[24] S.H.J. De Beukeleer, J.F. Janssens, H.O. Desseyn, J. Therm. Anal. 48 (1997) 225.
[25] K. Clou, J.F. Janssens, N. Blaton, A.T.H. Lenstra, H.O. Desseyn, Thermochim. Acta, accepted for publication.
[26] I. Wolfs, H.O. Desseyn, S.P. Perlepes, Spectrochim. Acta 50A (1994) 6, 1141.
[27] I. Wolfs, H.O. Desseyn, Spectrochim. Acta 52A (1996) 1521.